Simulations of Modal Active Control Applied to the Self-Sustained Oscillations of the Clarinet

Thibaut Meurisse,[a] Adrien Mamou-Mani,[b] and René Caussé[c]
UMR STMS IRCAM - CNRS - UPMC - 1 place Igor Stravinsky, 75004 Paris, France.

Baptiste Chomette[d]
CNRS - UMR 7190 - Institut Jean Le Rond d'Alembert, F-75005 Paris, France, and
UPMC - Université Pierre et Marie Curie 06 - Institut Jean Le Rond d'Alembert, F-75005 Paris, France.

David B Sharp[e]
The Open University - Walton Hall, Milton Keynes, MK7 6AA, UK.

(Dated: May 5, 2014)

This paper reports a new approach to modifying the sound produced by a wind instrument. The approach is based on modal active control, which enables adjustment of the damping and the frequencies of the different resonances of a system. A self-sustained oscillating wind instrument can be modeled as an excitation source coupled to a resonator via a non-linear coupling. The aim of this study is to present simulations of modal active control applied to a modeled self-sustained oscillating wind instrument in order to modify its playing properties. The modeled instrument comprises a cylindrical tube coupled to a reed and incorporates a collocated loudspeaker and microphone; it can thus be considered to approximate a simplified clarinet. Modifications of the pitch, the strength of the harmonics of the sound produced by the instrument, and of the oscillation threshold are obtained while controlling the first two resonances of the modeled instrument.

PACS numbers:

I. INTRODUCTION

Active control is a means of altering the sound and vibrations of a mechanical system by automatic modification of its structural response[1]. The important components for an active control set-up are a sensor to detect the vibration (usually a microphone for acoustical systems), a controller to manipulate the signal from the sensor, and an actuator to influence the response of the system (usually a loudspeaker for acoustical systems).

Two different approaches to active control are commonly used; the classical approach and the state-space approach[2].

The classical approach to active control is based on transfer functions and involves applying gains, phase shifting, filters and delays to the vibration signal measured by the sensor, and then sending the resultant signal to the actuator. Classical active control can be applied to a system either over specific frequency ranges or over the whole bandwidth, but it cannot modify the modal parameters of the individual resonances of the system in a targeted manner. Classical active control techniques were originally developed as a means of reducing vibrations in mechanical systems[3]. For example, using bandpass filters and time delays, self-sustained oscillating systems such as cavity flow oscillations can be controlled[4]. Musical wind instruments, such as the clarinet which can be modeled as an excitation (often referred to as a disturbance in the context of active control) coupled to a resonator via a non-linear coupling[5–8] (see Figure 1), are self-sustained oscillating systems. In principle, therefore, it is possible to apply classical active control techniques to wind instruments to modify their playing properties. Over the past decade, some preliminary work in this area has been carried out (this work has followed previous applications of classical active control to percussion and string instruments[10–12]). In particular, classical active control has been used to play a complete octave on a flute with no holes[13]. To achieve this, the incident wave was absorbed by a speaker at the end of the tube, and replaced by a chosen reflected wave. The classical approach has also been used to modify all the resonances of a simplified clarinet with gain and phase shifting[14], but the control could not modify the resonances independently.

The state-space approach to active control involves establishing a state space representation of the system. This is a mathematical model which, when projected on the modal base, represents the system in terms of state variables (expressed as vectors and matrices) containing the modal parameters (frequency, damping) of the system. Such a control is called modal active control[1]. Unlike the classical approach, modal active control enables the modal parameters of a system to be modified so that individual resonances can be adjusted to reach target frequency and damping values[15,21]. In

[a] Electronic address: thibaut.meurisse@ircam.fr
[b] Electronic address: adrien.mamou-mani@ircam.fr
[c] Electronic address: rene.causse@ircam.fr
[d] Electronic address: baptiste.chomette@upmc.fr
[e] Electronic address: david.sharp@open.ac.uk

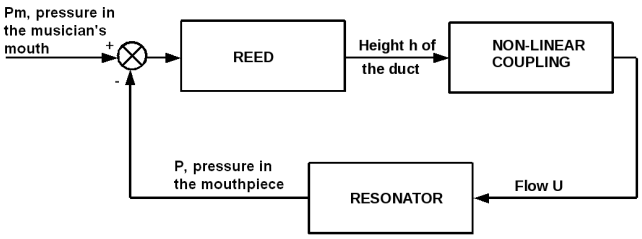

FIG. 1. Model of a self-sustained wind instrument[6,19].

principle, therefore, modal active control should enable the frequencies and the damping factors of the resonances of a wind instrument to be altered in a specified manner. However, the behavior of a self-sustained system with modal active control applied is unknown and needs to be investigated. There have been relatively few applications of modal active control to musical instruments[16,17] and no application to wind instruments to the authors' knowledge.

This paper reports a first step towards applying modal active control to real musical wind instruments. In this paper, simulations of modal active control applied to a model of a self-sustained simplified clarinet (i.e., a cylindrical tube coupled to a reed) are presented. The control is implemented with the intent of adjusting the resonances of the virtual instrument, thereby altering the timbre of the sound it produces as well as its playing properties. Such adjustments provide similar effects to those that would result from modifying the instrument's bore profile.

In Section II, a model of a simplified clarinet with an incorporated active control system is presented. The clarinet part of the model is made up of a reed model non-linearly coupled to a state-space model of the resonator. Meanwhile, the active control part of the model adds the components (microphone and loudspeaker) that are required to enable active control to be applied to the virtual instrument. In Section III, simulations are carried out to demonstrate the effects of the control. Four sets of simulations are presented. The first set provides examples of the control of the frequency and damping of the first resonance of the tube. The second and third sets provide maps showing control possibilities, in terms of both frequency and damping, for the first resonance of this self-sustained oscillating system. The fourth set provides an example of the control of the frequency and damping of the second resonance of the tube. Finally, Section IV provides some conclusions and outlines the proposed next steps for the research.

II. MODELING A SELF-SUSTAINED OSCILLATING WIND INSTRUMENT WITH INCORPORATED MODAL ACTIVE CONTROL SYSTEM

Models of self-sustained wind instruments such as the clarinet have been reported for over 30 years[5–8,18]. In such models, the instrument is described in terms of both linear (reed, resonator) and non-linear (coupling) elements (see Figure 1).
In this section, a complete model of a simplified clarinet with an incorporated modal active control system is developed (see Figure 2). First, a model of the clarinet reed and the non-linear coupling is described. Then, a state-space representation of the resonator is presented. This representation takes into account possible excitation both from the reed and from the speaker of the active control system, as well as monitoring of the pressure by the microphone of the active control system. Finally, the designs of the observer and controller elements of the active control system are described.

A. Reed and Non-Linear Coupling

The model of reed and non-linear coupling used in this paper is the one described by Karkar et al[8].
In a clarinet, a single reed controls the flow of air from the player's mouth into the instrument. Let $h(t)$ be the position of the reed at time t. Then,

$$\frac{1}{\omega_r^2}\ddot{h}(t) + \frac{q_r}{\omega_r}\dot{h}(t) + h(t) - h_0 = -\frac{1}{K_r}(P_m - P(t)) \quad (1)$$

where ω_r is the resonance frequency of the reed, q_r its damping, h_0 its equilibrium position and K_r its stiffness. The $\dot{}$ and $\ddot{}$ symbols represent respectively the first and second order time derivatives. P_m is the pressure in the player's mouth and $P(t)$ the pressure in the mouthpiece. Using the same assumptions as described in[19] and following Hirschberg[20], namely that:

- the flow is quasi-static,
- the kinetic energy of the flow is entirely dissipated by turbulence,
- the pressure is uniformly distributed in the mouthpiece and equal to that of the input of the resonator,
- the velocity of the air in the musician's mouth is negligible compared to that of the air in the flow,

the flow can be determined from

$$U(t) = H\big(h(t)\big)\,sign\big(P_m - P(t)\big)\,W h(t)\sqrt{\frac{2|P_m - P(t)|}{\rho_0}} \quad (2)$$

where W is the width of the reed duct and ρ_0 the density of the air. The Heaviside function $H(h(t))$ has been added to model the contact with the mouthpiece in order to deal with possible negative h values, which may happen numerically, but are not physical (they would involve the reed passing through the solid walls of the mouthpiece)[9]. In a previous paper[23], the Heaviside function

was not used and resulted in non-physical results.
To simplify the formulation of the equations, the following dimensionless parameters are introduced:

$$\begin{aligned} x_h(t) &= h(t)/h_0, \\ y_h(t) &= \dot{h}(t)/v_0, \\ p(t) &= P(t)/P_M, \\ u(t) &= U(t)Z_c/P_M \end{aligned} \tag{3}$$

where $v_0 = h_0\omega_r$ is characteristic of the reed's velocity during free motion, $P_M = K_r h_0$ is the pressure required to completely close the reed channel in static regime and $Z_c = \rho_0 c/S$ is the characteristic impedance of the tube with c the velocity of sound in the medium and S the section of the tube. The motion of the reed and the nonlinear coupling can therefore be described by the following equations:

$$\frac{1}{\omega_r}\dot{x}_h(t) = y_h(t), \tag{4a}$$

$$\frac{1}{\omega_r}\dot{y}_h(t) = 1 - x_h(t) + p(t) - \gamma - q_r y_h(t), \tag{4b}$$

$$u(t) = H\big(x_h(t)\big)\zeta sign\big(\gamma - p(t)\big)x_h(t)\sqrt{|\gamma - p(t)|} \tag{4c}$$

where $\zeta = Z_c W\sqrt{\frac{2h_0}{\rho_0 K_r}}$ is the dimensionless reed opening parameter and $\gamma = P_m/P_M$ represents the dimensionless pressure in the musician's mouth. Without control, the oscillation threshold is at $\gamma \simeq 1/3 + \epsilon$ with $\epsilon \ll 1$[7].

B. State-Space Model of the Resonator

Modal active control makes it possible to control the frequencies and damping factors of the modes of a system. To be able to apply modal active control, however, the system must be expressed in terms of a state-space model, comprising vectors and matrices which describe the system's modal parameters. Here, a state-space model of the resonator of the simplified clarinet is described. The model also incorporates the control system, with microphone (sensor) and speaker (actuator) included, as well as the disturbance (excitation) produced by the reed (see Section II.A).

The state-space model of the cylindrical tube used in this paper is derived in[15]. The diameter $2R$ of the tube is sufficiently small compared with its length L_t, that the tube can be considered to be a one-dimensional waveguide with spatial coordinate z, where $0 \le z \le L_t$. In the model, the speaker element of the control system is positioned at $z = z_s$, the microphone at $z = z_m$ and the disturbance is produced at $z = z_d$. They are all at the same position, at the input of the tube ($z_s = z_m = z_d = 0$).
The pressure in the tube, with the speaker incorporated in the tube wall and the reed at the entrance of the tube, is described by the nonhomogeneous equation:

$$\frac{1}{c^2}\ddot{p}(z,t) = p''(z,t) + \rho_0\dot{v}_s(t)\delta(z - z_s) + \frac{\rho_0}{SZ_c}\dot{u}(t)\delta(z - z_d) \tag{5}$$

where p is the dimensionless acoustic pressure, v_s the speaker baffle velocity, δ the Kronecker delta and u the dimensionless flow at the input of the instrument. The $'$ and $''$ symbols represent respectively the first and second order spatial derivatives. The second and third terms of the right-hand side of the equation represent respectively the contribution of the vibration of the control speaker and the contribution of the flow coming from the reed channel at the end of the tube.
Using separation of variables, let

$$p(z,t) = V(z)q(t) \tag{6}$$

and consider the homogeneous equation

$$\frac{1}{c^2}\ddot{p}(z,t) = p''(z,t). \tag{7}$$

Using equations (6) and (7) gives

$$V''(z) + \frac{\lambda}{c^2}V(z) = 0. \tag{8}$$

Hence,

$$V(z) = \alpha sin(kz) + \beta\cos(kz) \tag{9}$$

with $k^2 = \lambda/c^2$, where λ is a positive constant. As the tube is modeled as being closed at one end and open at the other, the following boundary conditions apply:

$$V(L_t) = 0, \tag{10}$$

$$V'(0) = 0. \tag{11}$$

This implies $\alpha = 0$ and $\cos(kL_t) = 0$, then $k_i = (2i - 1)\pi/2L_t$. Therefore

$$V_i(z) = \beta\cos(k_i z). \tag{12}$$

$V_i(z)$ is scaled so that

$$\begin{aligned} \left(V_i(z), \frac{1}{c^2}V_j(z)\right) &= \frac{1}{c^2}\int_0^{L_t} V_i(z)V_j(z)dz \\ &= \delta_{ij} \end{aligned} \tag{13}$$

where δ_{ij} is the Kronecker delta. This implies that

$$\beta = c\sqrt{\frac{2}{L_t}} \tag{14}$$

and thus

$$V_i(z) = c\sqrt{\frac{2}{L_t}}\cos(k_i z) \tag{15}$$

where $V_i(z)$ is the amplitude of the mode i at position z. Returning to the nonhomogeneous equation (5), let

$$p(z,t) = \sum_j V_j(z)q_j(t) \tag{16}$$

so that

$$\frac{1}{c^2}\sum_j \big[\ddot{q}_j(t) + \lambda_j q_j(t)\big]V_j(z) = \rho_0\dot{v}_s(t)\delta(z - z_s) + \frac{\rho_0}{SZ_c}\dot{u}(t)\delta(z - z_d) \tag{17}$$

where $\lambda_j = k_j^2 c^2$. Taking the inner product of both sides of (17) with $V_i(z)$ as in (10) and (11) yields

$$\ddot{q}_i + \lambda_i q_i(t) = b_i u_s(t) + g_i w(t) \tag{18}$$

where

$$u_s = \rho_0 \dot{v}_s \tag{19}$$

is the command sent to the speaker while the control system is operating, and

$$b_i = V_i(z_s) \tag{20}$$

with V_i described in eq.(15),

$$w(t) = \frac{\rho_0}{S Z_c} \dot{u} \tag{21}$$

is the disturbance signal sent by the reed through the non-linear coupling while the musician is blowing, and

$$g_i = V_i(z_d). \tag{22}$$

Equation 18 is the undamped normal mode equation for the cylindrical tube. To obtain a state-space description of the cylindrical tube with r modes, without considering the mode of the speaker, and including a proportional modal damping, let

$$\mathbf{x}(t) = \begin{bmatrix} q_i \\ \dot{q}_i \end{bmatrix}, \{i = 1...r\} \tag{23}$$

where $\mathbf{x}(t)$ is the state vector used in the linear model so that

$$\begin{aligned} \dot{\mathbf{x}}(t) &= \mathbf{A}\mathbf{x}(t) + \mathbf{B}u_s(t) + \mathbf{G}w(t), \\ y(t) &= \mathbf{C}\mathbf{x}(t) \end{aligned} \tag{24}$$

where u_s is defined in eq.(19), $w(t)$ is the disturbance signal at $z_d = 0$, $y(t)$ is the output of the system, the acoustic pressure measured at the position of the microphone so that

$$y(t) = p(z_m, t) = \sum_i V_i(z_m) q_i, \tag{25}$$

and

$$\mathbf{A} = \begin{bmatrix} 0_{r,r} & \mathbf{I}_{r,r} \\ -\mathrm{diag}(\omega_i^2) & -\mathrm{diag}(2\xi_i\omega_i) \end{bmatrix} \tag{26}$$

is the dynamical matrix which contains the frequencies and damping factors of the resonances of the cylindrical tube (with ω_i and ξ_i respectively denoting the frequency and the damping factor of the i^{th} mode). For a real instrument, over an infinite bandwidth, the dynamical matrix $\mathbf{A}$ is infinite with an infinite number of modes. In this paper, where a modeled instrument is studied over a limited bandwidth, the number of modeled modes is finite. The modal parameters of these modes are extracted from the input impedance of the tube, calculated using transmission matrices with electroacoustical analogues[26], using a Rational Fraction Polynomials (RFP) algorithm[25]. Meanwhile, $\mathbf{I}$ is the identity matrix. From eq.(18) and (19), it follows that

$$\mathbf{B} = \begin{bmatrix} 0_{r,1} \\ b_1 \\ \vdots \\ b_r \end{bmatrix}, \tag{27}$$

the actuator matrix with b_i described in eq.(20). From eq.(24) and (25), it follows that

$$\mathbf{C} = \begin{bmatrix} V_1(z_m) \cdots V_r(z_m) & 0_{1,r} \end{bmatrix}, \tag{28}$$

the sensor matrix with V_i described in eq.(15). Finally, from eq.(18) and (21), it follows that

$$\mathbf{G} = \begin{bmatrix} 0_{r,1} \\ g_1 \\ \vdots \\ g_r \end{bmatrix}, \tag{29}$$

the disturbance matrix with g_i decribed in eq.(22). As with the $\mathbf{A}$ matrix, the $\mathbf{B}$, $\mathbf{C}$ and $\mathbf{G}$ matrices are infinitely large for a real instrument. Here, where a modeled instrument is studied, they are finite in size.

C. Modal Control

Modal active control is used to modify the modal parameters of the resonances of a system. In other words, to modify their frequencies and damping factors.
To apply modal active control to the resonator of the simplified clarinet, a Luenberger[22] observer and a controller are implemented (see Figure 2). The observer directly receives what is measured by the microphone; its role is to rebuild the state vector $\mathbf{x}$ using a model of the system and the measurement $y = p$. Let $\mathbf{A}_m$, $\mathbf{B}_m$ and $\mathbf{C}_m$ be the modeled identified matrices of the system used by the observer. In this paper, the model used by the observer has the same number of modes as the clarinet model developed in Section II.B (thus $\mathbf{A}_m = \mathbf{A}$, $\mathbf{B}_m = \mathbf{B}$ and $\mathbf{C}_m = \mathbf{C}$). Meanwhile, let $\hat{\mathbf{x}}(t)$ be the built state vector estimated by the Luenberger observer. $\hat{\mathbf{x}}(t)$ is used by the controller to generate a command $u_s(t)$ that is transmitted through the speaker in order to apply the control to the resonator. This command $u_s(t)$, the same as in eq.(24), can be expressed as

$$u_s(t) = -\mathbf{K}\hat{\mathbf{x}}(t) \tag{30}$$

where $\mathbf{K}$ is the control gain matrix used to move the poles s_i of the system. $\mathbf{K}$ is determined, together with the $\mathbf{A}_m$ and $\mathbf{B}_m$ matrices, using a pole placement algorithm (in this work, the algorithm developed by Kautsky et al[27] is used).
The frequencies and damping factors of the resonator may be defined through the poles s_i of the $\mathbf{A}_m$ matrix, that is its eigenvalues, so that[2]:

$$\begin{aligned} Re(s_i) &= -\xi_i\omega_i, \\ Im(s_i) &= \pm\omega_i\sqrt{1-\xi_i^2}. \end{aligned} \tag{31}$$

By using control gains $\mathbf{K}$, these poles can be moved in order to reach new, target values for the resonator's frequencies (angular frequencies ω_{i_t}) and damping factors (ξ_{i_t}). These new poles are the eigenvalues of $\mathbf{A}_m - \mathbf{B}_m\mathbf{K}$. Control of this type is referred to as proportional state control. The dynamics of this observer can be written:

$$\begin{aligned}\dot{\hat{\mathbf{x}}}(t) &= \mathbf{A}_m\hat{\mathbf{x}}(t) + \mathbf{B}_m u_s(t) + \mathbf{L}(y(t) - \hat{y}(t)),\\ \hat{y}(t) &= \mathbf{C}_m\hat{\mathbf{x}}(t)\end{aligned} \tag{32}$$

where $\mathbf{L}$ is the observer gain vector. $\mathbf{L}$ is chosen such that the error between the measurement and its estimation, $e_y = y - \hat{y}$, converges to zero. It is calculated using a Linear Quadratic Estimator (LQE) algorithm. The $\hat{}$ symbol represents the estimations of the observer. $u_s(t)$ is calculated in eq.(30).
In the next section, transfer functions are carried out for both without control and with control (closed loop) conditions. Without control, the system of Figure 1 is described by :

$$\begin{aligned}\dot{\mathbf{x}}(t) &= \mathbf{A}\mathbf{x}(t) + \mathbf{G}w(t),\\ y(t) &= \mathbf{C}\mathbf{x}(t).\end{aligned} \tag{33}$$

The transfer function H_{WC} of such a system is then[24]:

$$H_{WC}(s) = \frac{y}{w} = \mathbf{C}(s\mathbf{I} - \mathbf{A})^{-1}\mathbf{G} \tag{34}$$

With control applied, the system of Figure 2 is described by eq.(24), (32) and (30). The closed loop transfer function H_{CL} is then[24]:

$$\begin{aligned}H_{CL}(s) &= \frac{y}{w}\\ &= \mathbf{C}(s\mathbf{I} - (\mathbf{A} - \mathbf{B}\mathbf{K}(s\mathbf{I} -\\ &\quad (\mathbf{A}_m - \mathbf{B}_m\mathbf{K} - \mathbf{L}\mathbf{C}_m))^{-1}\mathbf{L}\mathbf{C}))^{-1}\mathbf{G}\end{aligned} \tag{35}$$

The modal parameters of the transfer functions calculated with eq.(34) and (35) are extracted using a RFP algorithm, as for eq.(26).

The sounds and attack transients resulting from the simulations are also presented and discussed over the remainder of the paper.

III. SIMULATIONS

In order to validate the control and to observe its possible effects on the playing frequency, timbre and playability of notes produced by the modeled clarinet, a series of simulations is presented. The simulations are carried out using the Bogacki-Shampine method (*ode3* under *Simulink*) with a sample time of 1/44100 seconds, and a simulation time of 3 seconds.
In the simulations, the controlled resonator described by eq.(24), (30) and (32) is excited by a flow u (eq.(21)) obtained through the non-linear coupling (eq.(4c)) between it and the reed model (eq.(4a) and (4b)) on which a mouth pressure is applied. Figure 3 shows the shape of the dimensionless input pressure used. The resultant pressure generated within the resonator (cylindrical tube) is then fed back into the reed model and the non-linear coupling thereby ensuring the feedback between the reed and the resonator is accurately modeled.
In addition, the Luenberger observer measures the acoustic pressure at the input of the resonator throughout the simulation and reports to the controller which provides a second excitation for the resonator.
The characteristics of the modeled tube and reed are reported in table I[19]. Only the first 8 resonances of the tube are modeled.
Four sets of simulations are described. The first set provides examples of the control of the frequency and damping of the first resonance, in order to establish the efficiency of the control. The second and third sets provide maps which show the effects of the control of both the frequency and the damping of the first resonance, on the note produced by the virtual instrument. Finally, the fourth set provides an example of the control of the frequency and damping of the second resonance of the modeled tube, in order to verify the efficiency of the control on a resonance other than the first one. The effects of the control on the sound spectrum (calculated with the measured acoustic pressure) and the attack transient are studied. To emphasise their musical meaning, frequency differences are described in terms of cents (a semi-tone is 100 cents).

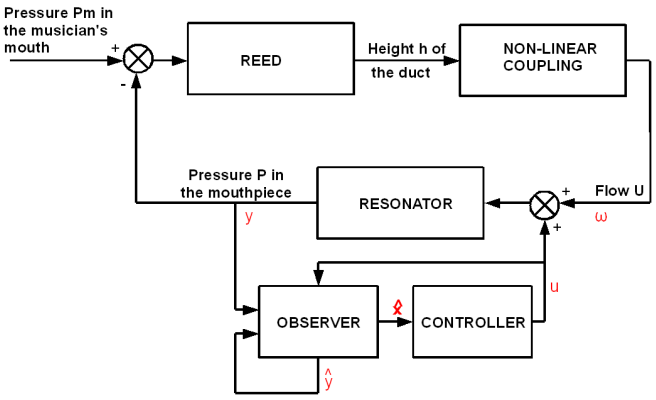

FIG. 2. Model of a self-sustained wind instrument with control system. w, y and u_s are defined in eq.(24). $\hat{y}$ and $\hat{\mathbf{x}}$ are the observer estimations of y and $\mathbf{x}$.

L_t	0.57m
R	0.007m
f_r	1500Hz
q_r	1
K_r	8×10^6N/m
h_0	3×10^{-4}m
W	0.015m

TABLE I. Parameters used to characterise the tube and the reed[19].

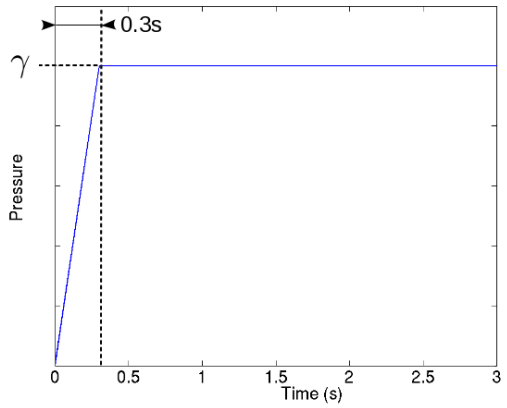

FIG. 3. Shape of the dimensionless pressure input used for the simulations.

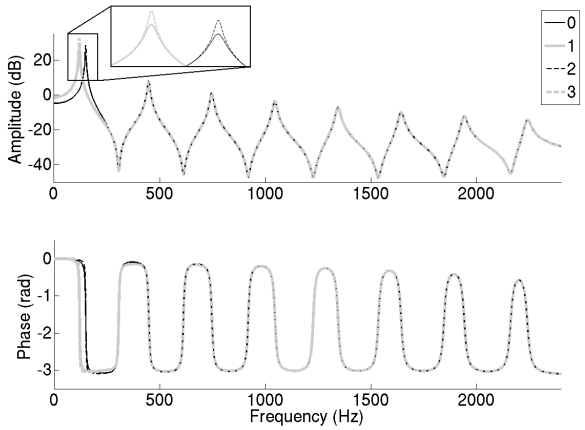

FIG. 4. Top : Transfer functions of the system in cases 0 (uncontrolled, solid black line), 1 (f_1 = 120Hz, solid grey line), 2 (ξ_{1_n} reduced by a factor of 2, dash black line) and 3 (f_1 = 120Hz and ξ_{1_n} reduced by a factor of 2, dash grey line). The transfer functions are calculated using eq.(34) (case 0) and eq.(35) (cases 1 to 3). Bottom : Phases of the transfer functions in cases 0 (solid black line), 1 (solid grey line), 2 (dash black line) and 3 (dash grey line).

A. Examples of Control of the Frequency and Damping of the First Resonance

In this first set of simulations, the efficiency of the control of the first resonance, in terms of both frequency and damping, is investigated. Four different cases are presented:

- Case 0 : No control;
- Case 1 : The control is applied with the intention of changing the frequency of the first resonance, from 149Hz to 120Hz;
- Case 2 : The control is applied with the intention of reducing the damping of the first resonance ξ_{1_n} by a factor of 2;
- Case 3 : The control is applied with the intention of changing the frequency of the first resonance, from 149Hz to 120Hz and reducing its damping by a factor of 2.

Figure 4 shows the transfer functions of the tube in the four cases. These transfer functions have been determined using eq.(34) (case 0) and eq.(35) (cases 1, 2 and 3) with the modal parameters extracted from calculated input impedance using an RFP algorithm. Table II shows the modal parameters of the first resonance of the transfer functions for the four cases. For cases 1 to 3, the table also shows the differences between the intended (target) frequencies and damping factors and the frequencies and damping factors that were actually observed. The controller is very accurate, with no error on the frequency and only 0.6% error for the damping. In all the cases, the amplitude is also affected with an increase of between 4.1dB (case 1) and 10.1dB (case 3). When the control changes the frequency (cases 1 and 3), the amplitude of the third resonance is also affected, with a decrease of 0.3dB.
Further explorations of the effects of the control have shown that increasing the frequency of the first resonance results in a decrease in its amplitude while decreasing the frequency of the first resonance results in an increase in its amplitude.

TABLE II. Modal parameters (frequency, amplitude, damping) of the first resonance of the transfer functions in figure 4 in cases 0 (uncontrolled), 1 (f_1 = 120Hz), 2 (ξ_{1_n} reduced by a factor of 2) and 3 (f_1 = 120Hz and ξ_{1_n} reduced by a factor of 2) and differences between attempted and obtained frequency and damping in cases 1 to 3. Frequencies and damping factors are extracted using a RFP algorithm.

Case	0	1	2	3
Frequency (Hz)	149	120	149	120
Differences (Cents)	NA	0	0	0
Damping	0.0179	0.0180	0.0089	0.009
Differences (%)	NA	0.6	0.6	0.6
Amplitude (dB)	22.5	26.6	28.5	32.6

Figure 5 shows the sound spectra of the steady-states of the sound produced by the system in the four cases, with a dimensionless mouth pressure γ = 0.4. With the control applied, the simulation still produces a sound whose pitch is based on the first resonance of the system. Envelopes are drawn on the four sound spectra to help illustrate the number of apparent harmonics (i.e., harmonics that are visible above the background noise level) in each sound. It can be seen that when the control is applied with the intention of changing the frequency of the first resonance (cases 1 and 3), the number of apparent harmonics in the sound spectrum is reduced. The reason for this is that the shifting of the first resonance frequency has caused it to be no longer harmonically related to the frequencies of the higher resonances. As a result, the upper harmonics in the sound are weakened. Conversely, when the control is applied with the intention of reducing the damping of

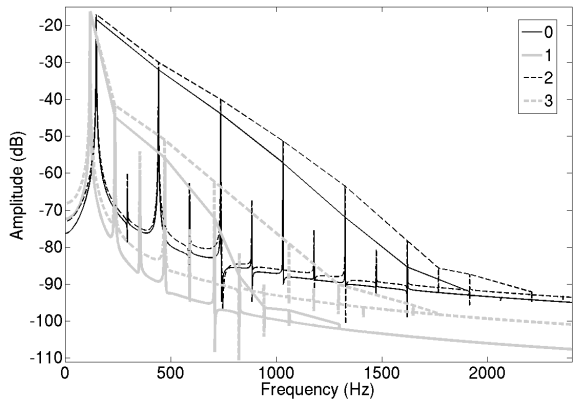

FIG. 5. Enveloped sound spectra of the self-sustained oscillating system in cases 0 (uncontrolled, solid black line), 1 (f_1 = 120Hz, solid grey line), 2 (ξ_{1_n} reduced by a factor of 2, dash black line) and 3 (f_1 = 120Hz and ξ_{1_n} reduced by a factor of 2, dash grey line), with $\gamma = 0.4$.

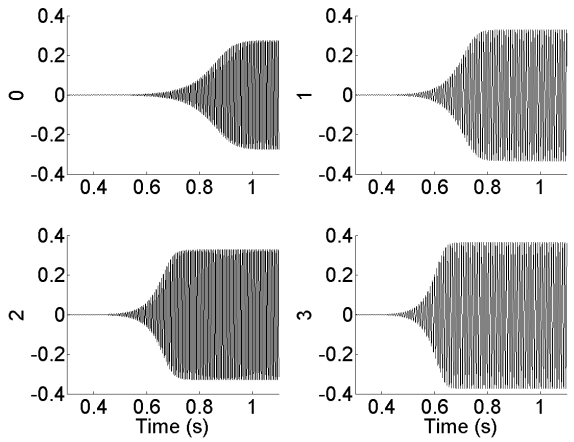

FIG. 6. Attack transients of the self-sustained oscillating system with $\gamma = 0.4$.
Top left : Case 0 (uncontrolled).
Top right : Case 1 ($f_1 = 120$Hz).
Bottom left : Case 2 (ξ_{1_n} reduced by a factor of 2).
Bottom right : Case 3 (f_1 = 120Hz and ξ_{1_n} reduced by a factor of 2).

the first resonance, the number of apparent harmonics in the sound is increased. It can be seen that the sound spectrum in case 2 has more apparent harmonics than the spectrum in case 0, and the sound spectrum in case 3 has more apparent harmonics than the spectrum in case 1. The effect of decreasing the damping is similar to that of increasing the mouth pressure. With the observed changes in the relative amplitudes of the harmonics in the sound spectra across the four cases, it is clear that the control has an effect (in terms of both intonation and timbre) on the sound produced by the virtual instrument.

Figure 6 shows the attack transients of the self-sustained system in the four cases, with $\gamma = 0.4$ (remember that in each case the mouth pressure applied to the reed model is as shown in Figure 3). It can be seen from Figure 6 that the attack transient is shorter in the cases where the control is applied; it is 1.05 seconds in duration when there is no control, 0.12s shorter (11% decrease) in case 1, 0.21s shorter (19% decrease) in case 2 and 0.34s shorter (31% decrease) in case 3. The amplitude of the signal is also affected, with increases of 19% (case 1 and 2) and 32% (case 3), but the waveform (not shown on the figure) is not affected. With the observed changes in the attack transient of the sound produced across the four cases, it is clear that the control has an effect on the onset of the note and appears to be affecting the playing characteristics of the virtual instrument.

B. Control of the Frequency of the First Resonance

This second set of simulations further explores the effects of the control on the frequency of the first resonance. In the simulations, the control is applied such that the frequency of the first resonance f_1 is varied from 20 Hz to 300 Hz in 1 Hz steps. For each frequency, the value of the dimensionless mouth pressure γ is varied from 0 (null pressure in the mouth of the musician) to 1 (the reed channel is closed in static regime) in 0.002 steps. In total, 140781 separate simulations are performed.
Figure 7 shows the entire search space covered by the simulations. The shaded regions correspond to conditions (first resonance frequencies and mouth pressure) which provide self-sustained oscillation. That is, conditions under which a note is produced. The depth of the shading (from light gray to black) indicates the playing frequencies of the note produced. (In this paper, the fundamental frequency of any given note produced by the virtual instrument is considered to be the playing frequency of that note.) The white regions correspond to conditions under which no note is produced. That is, conditions which do not support self-sustained oscillation. It can be seen that, provided the dimensionless mouth pressure is greater than approximately 0.4, stable solutions exist for all the first resonance frequencies tested in the simulations. This observation regarding the oscillation threshold (minimum mouth pressure which provides self-sustained oscillation) corroborates Section II.A.

Examination of Figure 7 reveals two main shaded regions; a black region in the bottom right corner of the map and a largely gray region in the top right corner of the map.
The black region corresponds to conditions that result in the playing frequency (and therefore the pitch) of the note produced by the virtual clarinet being based on the first resonance of the system. Broadly speaking, these conditions occur when the dimensionless mouth pressure falls in the range $0.34 < \gamma < 1$ and when the first resonance frequency falls in the range 20Hz $< f_1 <$ 196Hz. However, close inspection of the left hand side of the black region reveals that the oscillation

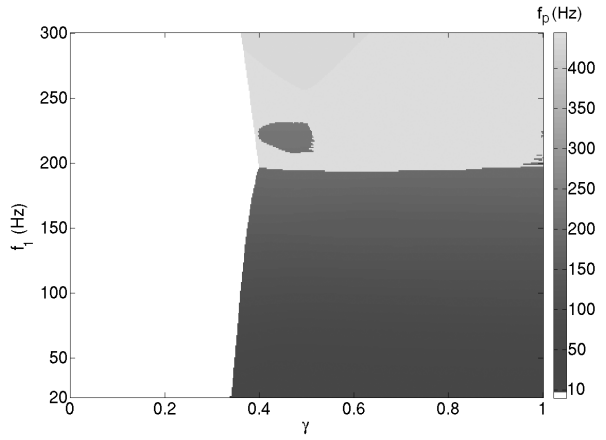

FIG. 7. Map of the playing frequencies f_p (indicated by the depth of shading) of the notes played by the simulations plotted with respect to the frequency of the first resonance f_1 (ordinate) and to the pressure in the mouth of the musician γ (abscissa). White regions correspond to conditions under which no note is produced.

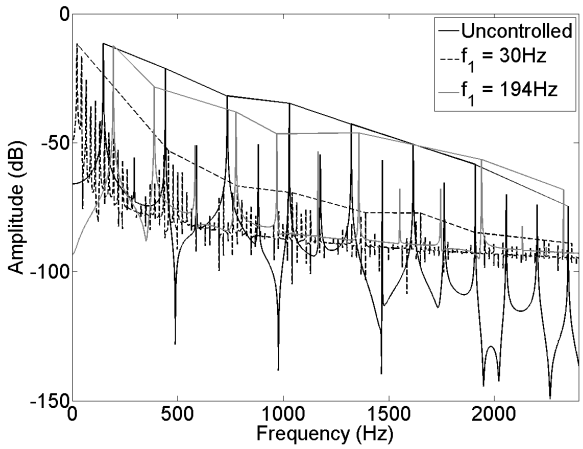

FIG. 8. Enveloped sound spectra of notes produced by the uncontrolled (solid black line) self-sustained oscillating system and by the system with 2 cases of control applied, $f_1 = 30$Hz (dash black line) and $f_1 = 194$Hz (solid gray line), and with $\gamma = 0.5$.

threshold (i.e., the mouth pressure at which the first non-white pixel is reached as one moves horizontally across the figure) actually increases from 0.34 to 0.4 as the frequency of the first resonance is increased. Within the black region, the playing frequencies range from 10 Hz to 194.3 Hz.

The gray region corresponds to conditions under which the playing frequency (and thus the pitch) of the note produced by the virtual clarinet becomes based on the second resonance of the system. (The effect is similar to that which results from opening a register key in a real wind instrument, where the amplitude of the first resonance is reduced and its frequency is altered so that there is no longer a harmonic relationship with the higher resonance frequencies[28].) In general, these conditions occur when the dimensionless mouth pressure falls in the range $0.362 < \gamma < 1$ and when the first resonance frequency falls in the range $197\text{Hz} < f_1 < 300\text{Hz}$. However, close inspection of the left hand side of the gray region reveals that the oscillation threshold actually decreases from 0.4 to 0.362 as the frequency of the first resonance is increased. Without any control applied, the first two resonance frequencies of the cylindrical tube are 149 Hz and 448 Hz respectively. The control is applied with the intention of shifting the first resonance frequency; the second resonance frequency of the resonator should remain unchanged at 448 Hz. However, within the gray region where the note produced is based on the second resonance of the system, the playing frequencies do not match this second resonance frequency exactly; instead they range from 434.9 Hz to 444.6 Hz.

Within the gray region of Figure 7, there is a small darker region corresponding to specific conditions where the playing frequency (pitch) of the note produced by the virtual clarinet once again becomes based on the first resonance frequency of the instrument. These conditions occur when the dimensionless mouth pressure is in the range $0.474 < \gamma < 0.516$ and when the first resonance frequency is in the range $208\text{Hz} < f_1 < 224\text{Hz}$. The reason that the playing frequency becomes based on the first resonance frequency under these conditions can be understood if it is recalled that the resonator of the virtual instrument is a closed-open cylindrical tube. Without control applied, the frequencies of the first two resonances of the tube have a harmonic relationship, with $f_2 = 3 \times f_1$. When the control is applied, the frequency of the first resonance is altered so that, in general, it no longer has a harmonic relationship with the higher resonance frequencies. However, under the conditions corresponding to the small darker region, the first resonance frequency is shifted upwards such that the frequencies of the first two resonances of the tube are once more approximately harmonically related, with now $f_2 = 2 \times f_1$.

Figure 8 shows the sound spectra of three notes obtained from the simulations with a dimensionless mouth pressure of $\gamma = 0.5$; with no control applied and with control applied to give first resonance frequencies of 30 Hz and 194 Hz.

When $f_1 = 30$Hz, the playing frequency of the note is based on the first resonance of the system. The low first resonance frequency results in closely spaced harmonics in the spectrum. However, these harmonics tend to be low in amplitude because the majority are not supported by the higher resonances of the tube (which are not harmonically related in frequency to the first tube resonance). It is only when the frequencies of the harmonics happen to coincide with those of the higher resonances of the tube (at around 448 Hz, for example, which is the second resonance frequency) that their amplitudes become greater. It should be noted that in the simulations, the dynamics of the loudspeaker are not modeled. This makes it possible to alter the first

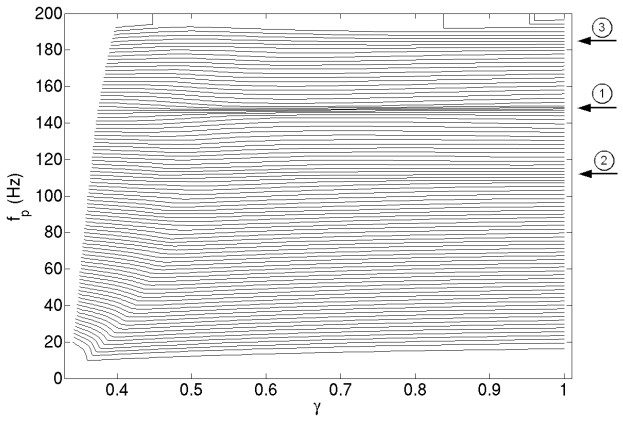

FIG. 9. Playing frequencies f_p observed in the black region of Figure 7 (20Hz $< f_1 <$ 196Hz) plotted with respect to the mouth pressure γ. Each line stands for a single value of f_1 (i.e., a single target first resonance frequency). The first arrow indicates a region such that $f_1 \approx f_2/3$, the second arrow indicates a region around $f_1 \approx f_2/4$, and the third arrow indicates a region around $f_1 \approx f_3/4$.

resonance frequency by such a large amount and still produce a sound. In reality, the loudspeaker dynamics will prevent the control from achieving such a large degree of variation of the resonance frequencies.
When $f_1 = 194$Hz with a mouth pressure of $\gamma = 0.5$, the playing frequency is based on the first resonance of the system, and it is at the edge of the register change. The high first resonance frequency results in an increase in the frequency separation of the harmonics in the spectrum. It can be seen that at lower frequencies (under 1650 Hz), these harmonics have a lower amplitude compared to the uncontrolled system, because they are not supported by the higher resonances of the tube (which are not harmonically related in frequency to the first tube resonance). At higher frequencies, especially for the harmonics with frequency 1940 Hz and 2328 Hz, this amplitude becomes higher compared to the system with no control, suggesting that these harmonics may coincide in frequency with (and hence be supported by) higher resonances of the tube.

Figure 9 shows the playing frequencies f_p observed in the black region of Figure 7 (20Hz $< f_1 <$ 196Hz) plotted with respect to the mouth pressure γ. Each line corresponds to a single value of f_1 (i.e., a single target first resonance frequency) and the lines go up in 2Hz steps. Figure 9 therefore shows the behaviour of the system when the mouth pressure is increased. There are three zones where the lines converge, highlighted by arrows on the right side of the figure.
The region indicated by the first arrow corresponds to a frequency range where the controlled f_1 is approximately harmonically related to the other resonances of the tube (that is, $f_2 = 3 \times f_1$, $f_3 = 5 \times f_1$, and so on). Therefore over this range the reed will be strongly supported (by all the resonances) in opening and closing at a rate approximately equal to $f_2/3$, that is at a frequency close to the value of f_1 when no control is applied. Therefore, the playing frequency f_p in this region is approximately equal to $f_2/3$.
Similarly, the region indicated by the second arrow corresponds to a frequency range where the controlled f_1 is approximately harmonically related to the second resonance of the tube ($f_2 = 4 \times f_1$). Over this range the reed will be strongly supported (by both the first and second resonances) in opening and closing at a rate approximately equal to $f_2/4$. Therefore, the playing frequency f_p in this region is approximately $f_2/4$.
And the region indicated by the third arrow corresponds to a frequency range where the controlled f_1 is approximately harmonically related to the third resonance of the tube ($f_3 = 4 \times f_1$). For this frequency range, the reed will be strongly supported by the first and third resonances in opening at a rate approximately equal to $f_3/4$. Therefore, the playing frequency f_p in this region is approximately $f_3/4$.

C. Control of the Damping of the First Resonance

This third set of simulations further explores the effects of the control on the damping of the first resonance. In the simulations, the control is applied such that the natural damping of the first resonance ξ_{1_n} is:

- Increased by factors from 0 to 1.15 (times the natural damping (ξ_{1_n})) in 0.05× steps;
- Increased by factors from 1.2 to 5.4 in 0.2× steps;
- Increased by factors from 5.5 to 10.5 in 0.5× steps;
- Increased by factors from 11 to 20 in 1× steps.

For each damping value, the value of the dimensionless mouth pressure γ is varied from 0 (null pressure in the mouth of the musician) to 1 (the reed channel is closed in static regime) in 0.002 steps. In total, 33567 separate simulations are performed.
Figure 10 shows the entire search space covered by the simulations. As before, the shaded regions correspond to conditions (first resonance frequencies and mouth pressure) which provide self-sustained oscillation. That is, conditions under which a note is produced. The depth of the shading (from light gray to black) indicates the playing frequencies of the note produced. The white regions correspond to conditions under which no note is produced. That is, conditions which do not support self-sustained oscillation. It can be seen that, provided the dimensionless mouth pressure is greater than approximately 0.4, stable solutions exist for all the first resonance damping factors tested in the simulations. This observation regarding the oscillation threshold also corroborates Section II.A.

Examination of Figure 10 reveals two main shaded regions; a black region in the bottom right corner of the map and a large gray region in the top right corner of the map.

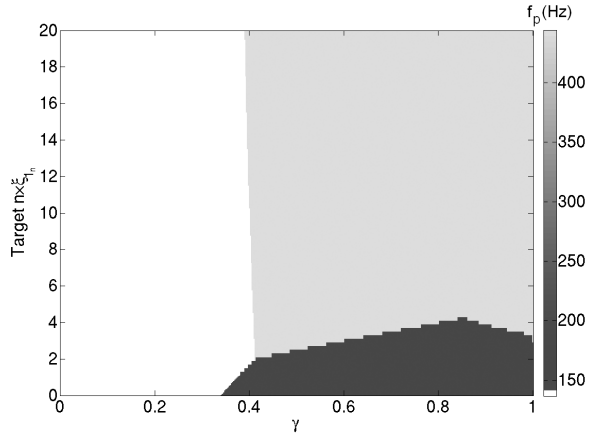

FIG. 10. Map of the playing frequencies (indicated by the depth of shading) of the notes played by the simulations plotted with respect to the target modification of the damping of the first resonance (ordinate, $\xi_1 = value \times \xi_{1_n}$) and to the pressure in the mouth of the musician γ (abscissa). White regions correspond to conditions under which no note is produced.

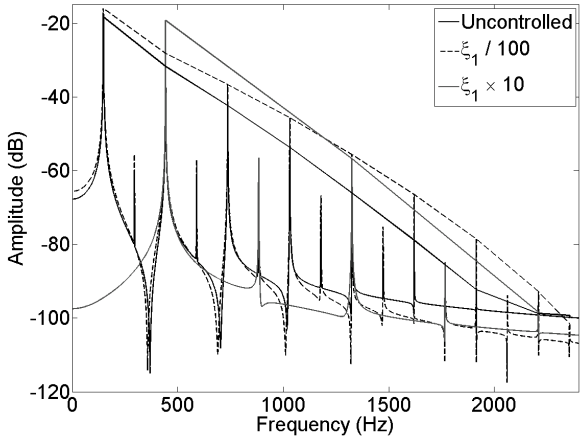

FIG. 11. Enveloped sound spectra of notes produced by the uncontrolled (solid black line) self-sustained oscillating system and by the system with 2 cases of control applied, ξ_{1_n} reduced by a factor of 100 (dash black line) and ξ_{1_n} increased by a factor of 10 (solid gray line), and with $\gamma = 0.41$.

The black region corresponds to conditions that result in the playing frequency (and therefore the pitch) of the note produced by the virtual clarinet being based on the first resonance of the system. Broadly speaking, these conditions occur when the dimensionless mouth pressure falls in the range $0.34 < \gamma < 1$ and when the first resonance damping factor falls in the range $0 \times \xi_{1_n} < \xi_1 < 4.2 \times \xi_{1_n}$. However, close inspection of the left hand side of the black region reveals that the oscillation threshold (i.e., the mouth pressure at which the first non-white pixel is reached as one moves horizontally across the figure) actually increases from 0.34 to 0.41 as the damping of the first resonance is increased. Within the black region, the playing frequencies range from 146.7 Hz to 147.9 Hz, which is a little under the frequency of the first resonance, 149 Hz.

The gray region corresponds to conditions under which the playing frequency (and thus the pitch) of the note produced by the virtual clarinet becomes based on the second resonance of the system. In general, these conditions occur when the dimensionless mouth pressure falls in the range $0.39 < \gamma < 1$ and when the first resonance damping factor falls in the range $2 \times \xi_{1_n} < \xi_1 < 20 \times \xi_{1_n}$. However, close inspection of the left hand side of the gray region reveals that the oscillation threshold actually decreases from 0.41 to 0.39 as the damping of the first resonance is increased. Within the gray region the playing frequencies range from 440.3 Hz to 444 Hz, which is close to the frequency of the second resonance, 448 Hz.

The black region extends up to a damping value of $4.2 \times \xi_{1_n}$ at a mouth pressure $\gamma = 0.85$. This is the largest damping value possible before a change in register occurs. Indeed, at this point, increasing or decreasing the mouth pressure results in a register change from the first register to the second register (i.e., the playing frequency (and thus the pitch) of the note produced by the virtual clarinet becomes based on the second resonance).

Figure 11 shows the sound spectra of three notes obtained from the simulations with a dimensionless mouth pressure of $\gamma = 0.41$; with no control applied and with control applied to give first resonance damping factors reduced by a factor of 100, and increased by a factor of 10.

When ξ_{1_n} is reduced by a factor of 100, the playing frequency of the note is based on the first resonance of the system. Reducing the damping in this way results in an increase of the amplitude of all the harmonics (from +2.5dB to +12.5dB), with one more apparent harmonic (i.e., harmonic that is visible above the background noise level). This effect is similar to increasing the mouth pressure.

When ξ_{1_n} is increased by a factor of 10, the playing frequency of the note is based on the second resonance of the system. The last apparent harmonic in the sound spectrum is the same as for the sound produced with no control applied, but as the playing frequency is now based on the second resonance of the system, the number of harmonics in the spectrum is decreased by a factor of 3.

D. Example of Control of the Frequency and Damping of the Second Resonance

Sections III.A, III.B and III.C explored the effects of the control of the frequency and damping of the first resonance of the modeled tube. It is also possible to apply the active control to the other tube resonances.

In this fourth set of simulations, an example of the control of the second resonance, in terms of both frequency

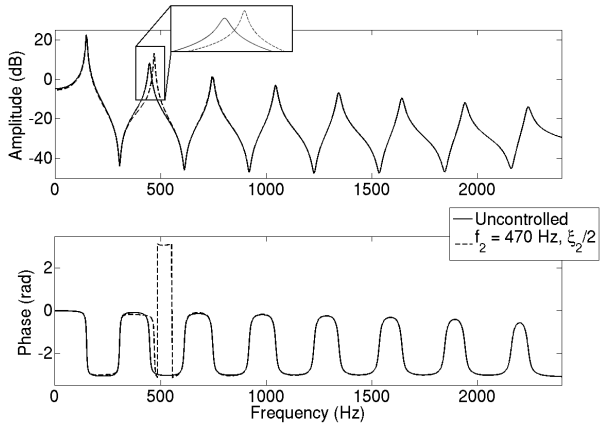

FIG. 12. Top : Transfer functions of the system without control (solid black line) and with control applied with the aim of modifying the frequency of the second resonance, from $f_2 = 448$Hz to $f_2 = 470$Hz and reducing its damping by a factor of 2 (dash black line). Bottom : Phases of the transfer functions with no control (solid black line) and with control applied (dash black line).

and damping, is presented. The control is applied with the intention of modifying the frequency of the second resonance from $f_2 = 448$Hz to $f_2 = 470$Hz and reducing its damping value by a factor of 2.

Figure 12 shows the transfer functions of the uncontrolled tube and the tube with control applied. These transfer functions have been determined using eq.(34) (uncontrolled tube) and eq.(35) (control applied) with the modal parameters extracted from the calculated input impedance using an RFP algorithm. Table III shows the modal parameters of the first 8 resonances of the transfer functions without control and with control applied. The table also shows the differences between the intended (target) frequencies and damping factors and the frequencies and damping factors that were actually observed. Modifications of the amplitude due to the control are also observed. As only the second resonance is controlled, for all the other seven resonances the intended values are the same as the values when uncontrolled. The controller is very accurate for the frequency and damping, with no error on the frequency of the controlled resonance and no more than 3% error for the damping. The amplitude of the controlled resonance is however affected with an increase of 5dB. The amplitude of all the other resonances is also affected with a decrease of 0.7dB of the first resonance, and increases of between 0.1dB (resonances 6 to 8) and 0.6dB (resonance 3).

Figure 13 shows the sound spectra of the steady-states of the sound produced by the system when uncontrolled and with the control applied, with a dimensionless mouth pressure $\gamma = 0.4$. With the control applied, the simulation still produces a sound whose pitch is based on the first resonance of the system. However, it can be seen that with the control, the number of

TABLE III. Modal parameters (frequency, amplitude, damping) of the resonances of the transfer functions (figure 12) of the uncontrolled (U) and controlled (C) tubes and differences between intended (T) and obtained values. For resonances 1 and 3 to 8, intended values and values when uncontrolled are the same. Frequencies and damping are extracted using a RFP algorithm.

Resonance		1	2	3	4
Frequency (Hz)	U	149	448	746	1046
	C	149	470	746	1046
			(T : 470)		
Difference (cents)		0	0	0	0
Damping	U	0.0178	0.0105	0.0082	0.0071
	C	0.0178	0.0055	0.0083	0.0072
			(T : 0.0053)		
Difference (%)		0	3	1	1
Amplitude (dB)	U	22.5	8.1	1.3	-3.3
	C	21.8	13.1	1.9	-3
Difference (dB)		-0.7	+5	+0.6	+0.3

Resonance		5	6	7	8
Frequency (Hz)	U	1344	1643	1942	2242
	C	1344	1643	1942	2242
Difference (cents)		0	0	0	0
Damping	U	0.0065	0.006	0.0057	0.0054
	C	0.0067	0.0059	0.0056	0.0053
Difference (%)		1	1	1	1
Amplitude (dB)	U	-6.8	-9.6	-12	-14
	C	-6.6	-9.5	-11.9	-13.9
Difference (dB)		+0.2	+0.1	+0.1	+0.1

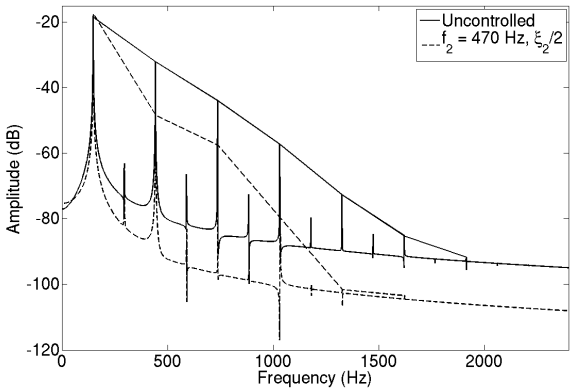

FIG. 13. Enveloped sound spectra of the notes produced by the self-sustained oscillating system without control (solid black line) and with control applied with the aim of modifying the frequency of the second resonance, from $f_2 = 448$Hz to $f_2 = 470$Hz and reducing its damping by a factor of 2 (dash black line), with $\gamma = 0.4$.

apparent harmonics (i.e., harmonics that are visible above the background noise level) in the sound spectrum is reduced. The reason for this is that the shifting of the second resonance frequency has caused it to be no longer harmonically related to the frequency of the first resonance. As a result, the strength of the second harmonic in the sound is weakened, as well as the strength of the upper harmonics. With the observed

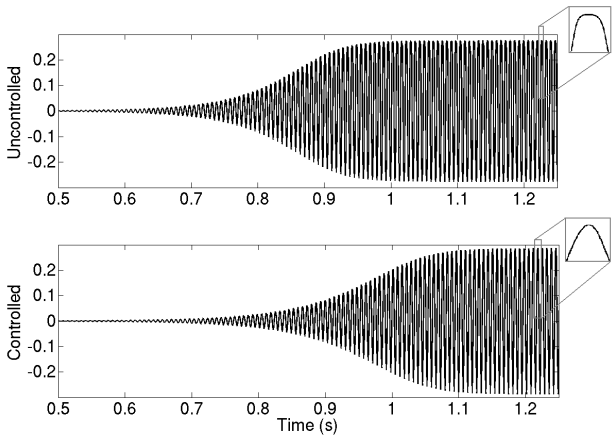

FIG. 14. Attack transients of the self-sustained oscillating system with $\gamma = 0.4$. Top: uncontrolled. Bottom: control applied with the aim of modifying the frequency of the second resonance, from $f_2 = 448$Hz to $f_2 = 470$Hz and reducing its damping by a factor of 2.

changes in the relative amplitudes of the harmonics in the sound spectra, it is clear that the control of the second resonance also has an effect (in terms of timbre) on the sound produced by the virtual instrument.

Figure 14 shows the attack transients of the self-sustained system when uncontrolled and with the control applied, with $\gamma = 0.4$ (the mouth pressure applied to the reed model is as shown in Figure 3). Remember that even with the control applied, the model still produces a sound whose pitch is based on the first resonance of the system. It can be seen from Figure 14 that the attack transient is longer when the control is applied; it is 1.05 seconds in duration when there is no control, 0.12s longer (11% increase) when the control is applied. The amplitude of the signal is also affected, with an increase of 4%, and the waveform is modified, from a square-like signal to a more sinusoidal-shaped signal. With the observed changes in the attack transient of the sound produced, it is clear that the control of the second resonance also has an effect on the onset of the note and appears to be affecting the playing characteristics of the virtual instrument.

IV. CONCLUSION AND PERSPECTIVES

In this paper, simulations of modal active control using linear quadratic estimator and pole placement algorithms applied to a model of a self-sustained simplified clarinet in order to modify its emitted sound and playability have been presented. To the authors' knowledge, it is the first time that such a control has been applied to a self-sustained system. Effects of this control have been studied with four sets of simulations. Modifications were observed of:

- the pitch of the sound produced by the instrument,
- the strength of the harmonics of the sound,
- the oscillation threshold.

The controller has been shown to be very accurate with respect to the control of the damping and frequency of the first resonance. Similar levels of accuracy have been demonstrated when controlling a higher resonance (the second resonance), although in this case the control led to unintended modifications of the amplitudes of the uncontrolled resonances. Meanwhile, the control of the first and second resonances has been shown to lead to modifications in the sound spectra and attack transients of notes produced by the modeled simplified clarinet. The harmonics in the sound spectra were observed to be weakened as a result of either frequency changes or increases in damping of the resonances, and strengthened as a result of decreases in damping. Moreover, large increases in the frequency and/or damping of the first resonance resulted in a reduction in its amplitude leading to a change in the register of the note produced. This effect is the same as that resulting from opening a register hole in a real wind instrument.

Although the simulations have demonstrated the great potential of modal active control for modifying the frequencies and damping values of the resonances of a wind instrument, it should be noted that no consideration has so far been given to the dynamics of the loudspeaker used to apply the control. These loudspeaker dynamics will place restrictions on the extent to which the frequencies and damping values of a given resonance can be modified. It is planned to take into account the loudspeaker properties in the simulations in order to make them more realistic. A study of the limits and possibilities of the control of all the resonances (i.e., the limits of the pole placement with respect to the mouth pressure) will then be carried out. In addition, the optimal positions of the sensor (microphone) and actuator (loudspeaker) will be investigated. It is then planned to apply the control to a real simplified instrument.

Acknowledgments

This work was carried out during the PhD of Thibaut Meurisse, funded by Agence Nationale de la Recherche (ANR IMAREV project) and Université Pierre et Marie Curie (UPMC, Paris 6). We thank gratefully Sami Karkar and Fabrice Silva for their help with their clarinet model. We also thank Simon Benacchio for his support about the LQE algorithm. We thank the Newton International Fellowship scheme for funding the collaboration between France and UK.

APPENDIX A: NOMENCLATURE

$\dot{}$ = First order time derivative
$\ddot{}$ = Second order time derivative
$'$ = First order spatial derivative
$''$ = Second order spatial derivative
$\mathbf{A}$ = System matrix
$\mathbf{A}_m$ = Modeled system matrix for the observer
b_i = Amplitude of the mode i at speaker position
$\mathbf{B}$ = Actuator matrix
$\mathbf{B}_m$ = Modeled actuator matrix for the observer
c = Velocity of sound in the medium
$\mathbf{C}$ = Sensor matrix
$\mathbf{C}_m$ = Modeled sensor matrix for the observer
f_p = Playing frequency
f_r = Resonance frequency of the reed
$\mathbf{G}$ = Disturbance matrix
$h(t)$ = Position of the reed
h_0 = Equilibrium position of the reed
H_{CL} = Closed-loop transfer function
H_{WC} = Without control transfer function
$\mathbf{K}$ = Control gain matrix
K_r = Stiffness of the reed
$\mathbf{L}$ = Observation gain vector
L_t = Length of the tube
$p(t)$ = Dimensionless version of $P(t)$
$p(z,t)$ = Acoustic pressure in the tube
$P(t)$ = Pressure in the mouthpiece
P_m = Pressure in the player's mouth
P_M = Pressure required to completely close the reed channel in static regime
$q(t)$ = Time component of $p(z,t)$
q_r = Damping of the reed
R = Radius of the tube
s = Laplace variable
s_i = Pole i
s_{i_t} = Target pole i
S = Cross-sectional area of the tube
$u(t)$ = Dimensionless version of $U(t)$
$u_s(t)$ = Control command
$U(t)$ = Flow through the reed duct
v_0 = Reed velocity in free behavior
$v_s(t)$ = Speaker baffle velocity
$V(z)$ = Spatial component of $p(z,t)$
$V_i(z)$ = Amplitude of the mode i at position z
$w(t)$ = Disturbance signal
W = Width of the reed duct
$\mathbf{x}(t)$ = State vector
$\hat{\mathbf{x}}$ = Observer estimation of $\mathbf{x}(t)$
$x_h(t)$ = Dimensionless version of $h(t)$
$y(t)$ = Output of the system
$\hat{y}$ = Observer estimation of $y(t)$
$y_h(t)$ = Dimensionless version of $\dot{h}(t)$
z = Spatial coordinate
z_d = Position of the disturbance
z_m = Position of the microphone
z_s = Position of the speaker
Z_c = Characteristic impedance of the tube
α = Constant
β = Constant
γ = Dimensionless version of P_m
δ = Kronecker delta
ζ = Dimensionless reed opening parameter
λ = Positive constant
ξ_i = Damping of mode i
ξ_{i_t} = Targeted damping for mode i
ρ_0 = Density of the acoustic medium
ω = Angular frequency
ω_i = Angular frequency of mode i
ω_{i_t} = Targeted angular frequency for mode i
ω_r = Angular resonance frequency of the reed

[1] C.R. Fuller, S.J. Elliott and P.A. Nelson, *Active Control of Vibration* (Academic Press, Harcourt Brace and Company, London, 1996, reprinted 1997), Chap.3, pp.59-90.
[2] A.Preumont, *Vibration Control of Active Structures, An Introduction - Third Edition* (Springer, Verlag Berlin Heidelberg, 2011), 1-432, p.197.
[3] PA. Nelson, SJ. Elliot, *Active Control of Sound* (Academic Press, Harcourt Brace and Company, London, 1992, reprinted 1995), 1-436.
[4] C.W. Rowley, D.R. Williams, T. Colonius, R.M. Murray, D.G. Macmynowski, "Linear models for control of cavity flow oscillation", J. Fluid Mech, **547**, 317-330 (2006).
[5] R. T. Schumacher, "Self-Sustained Oscillations of the Clarinet: An Integral Equation Approach", ACUSTICA, **40**, 298-309 (1978).
[6] M. E. McIntyre, R. T. Schumacher, J. Woodhouse, "On the oscillations of musical instruments", J. Acoust. Soc. Am., **74**(5), 1325-1345 (November 1983).
[7] F. Silva, J. Kergomard, C. Vergez, J. Gilbert, "Interaction of reed and acoustic resonator in clarinetlike systems", J. Acoust. Soc. Am., **124**(5), 3284-3295 (November 2008).
[8] S. Karkar, C. Vergez, B. Cochelin, "Oscillation threshold of a clarinet model: A numerical continuation approach", J. Acoust. Soc. Am., **131**(1), 698-707 (January 2012).
[9] S. Karkar, C. Vergez, B. Cochelin, "Toward the systematic investigation of periodic solutions in single reed woodwind instruments", Proc. of the 20th Int. Symp. on Music Acousticas, Associated Meeting of the International Congress on Acoustics, International Commission fos Acoustics, Sydney, Australia, 1-7 (2010).
[10] C. Besnainou, "Modal Stimulation : a Sound Synthesis New Approach", Proc. of the Int. Symp. on Music Acoustics 1995, Dourdan, France, 434-438 (1995).
[11] H. Boutin, *Méthodes de contrôle actif d'instruments de musique. Cas de la lame de xylophone et du violon.* (Musical instruments active control methods. Cases of the xylophone bar and of the violin.) (Phd Thesis, Université Pierre et Marie Curie - Paris VI, 2011).
[12] E. Berdahl, J. Smith, "Feedback control of acoustic musical instruments: Collocated control using physical analogs", J. Acoust. Soc. Am., **131**, 963-973 (2012).
[13] J. Guérard, *Modélisation numérique et simulation expérimentale de systèmes acoustiques - Application aux instruments de musique.* (Digital modeling and experimental simulation of acoustical systems - Application to musical instruments.) (Phd Thesis, Université Pierre et Marie Curie - Paris VI, 2002).
[14] T. Meurisse, A. Mamou-Mani, R. Caussé, D. Sharp, "Active control applied to simplified wind musical instrument", Proc. Int. Cong. on Acoustics 2013, **19**, 2pEAb7,

Montréal, Canada (2-7 June 2013).
[15] J. Hong, J.C. Akers, R. Venugopal, M-N. Lee, A.G. Sparks, P.D. Washabaugh, D.S. Bernstein , "Modeling, Identification, and Feedback Control of Noise in an Acoustic Duct," IEEE Transactions on Control Systems Technology, **4**(3), 283-291 (May 1996).
[16] S. Hanagud, S. Griffin, "Active Structural Control for a Smart Guitar," Proc. of the 4th European Conference On Smart Structures and Materials, Harrogate, United Kingdom, 1-7 (July 6-8 1998).
[17] S. Benacchio, A. Mamou-Mani, B. Chomette, F. Ollivier, "Simulated Effects of Combined Control Applied to an Experimentally Identified Soundboard," Proc. of the Stockholm Music Acoustics Conference 2013 (SMAC 2013), Stockholm, Sweden, 601-606 (August 2013).
[18] F. Silva, *Emergence des auto-oscillations dans un instrument de musique à anche simple.* (Appearance of self-sustained oscillation in a single reed musical instrument.) (Phd Thesis, Université de Provence - Aix-Marseille I, 2009).
[19] S. Karkar, *Méthodes numériques pour les systèmes dynamiques non linéaires - Application aux instruments de musique auto-oscillants.* (Digital methods for non linear dynamical systems - Application to self-sustained oscillated musical instruments.) (Phd Thesis, Université de Provence - Aix-Marseille I, 2012).
[20] A. Hirschberg : *Aero-Acoustics of Wind Instruments*, in G.Weinreich, A.Hirschberg, J.Kergomard, *Mechanics of Musical Instruments*, volume 335 of CISM Courses and Lectures. Springer-Verlag, Wien - New York (1995), 291-369.
[21] B. Chomette, D. Remond, S. Chesné, and L. Gaudiller, "Semi-adaptive modal control of on-board electronic boards using identication method", Smart Material and Structures, **17**(6), 1-8 (2008).
[22] D. Luenberger, "An introduction to Observers," IEEE Transactions on Automatic Control, **16**(6), 596-602 (1971).
[23] T. Meurisse, A. Mamou-Mani, R. Caussé, D. Sharp, "Simulations of Modal Active Control Applied to the Self-Sustained Oscillations of the Clarinet," Proc. of the Stockholm Music Acoustics Conference 2013 (SMAC 2013), Stockholm, Sweden, 425-431 (30 July - 3 August 2013).
[24] B. Chomette, S. Chesné, D. Rémond, L. Gaudiller, "Damage reduction of on-board structures using piezoelectric components and active modal control - Application to a printed circuit board", Mechanical Systems and Signal Processing, **24**, 352-364 (2010).
[25] T. Richardson, D. Formenti, "Parameter estimation from frequency response measurements using rational fraction polynomials", First International Modal Analysis Conference (1eIMAC), Orlando, USA, 167-180 (1982).
[26] M. Rossi, *Traité d'électricité, Volume XXI, Électroacoustique* (Electricity tract, Volume 21, Electroacoustic), (Presses polytechniques romandes, première édition, Lausanne, 1986), Chap.5, pp.185-232.
[27] J. Kautsky, N.K. Nichols, "Robust Pole Assignment in Linear State Feedback", Int. J. Control, **41**, 1129-1155 (1985).
[28] A. Mamou-Mani, D. Sharp, T. Meurisse, W. Ring, "Investigating the consistency of woodwind instrument manufacturing by comparing five nominally identical oboes", J. Acoust. Soc. Amer., **131**(1), 728-736 (January 2012).